

# Lasing-induced reduction in core heating in high wall plug efficiency quantum cascade lasers

Anthony J. Hoffman,<sup>1,a)</sup> Phillip X. Braun,<sup>1</sup> Matthew D. Escarra,<sup>1</sup> Scott S. Howard,<sup>1,b)</sup> Kale J. Franz,<sup>1</sup> Xiaojun Wang,<sup>2</sup> Jenyu Fan,<sup>2</sup> and Claire Gmachl<sup>1</sup>

<sup>1</sup>Department of Electrical Engineering, Princeton University, Princeton, New Jersey 08544, USA

<sup>2</sup>Adtech Optics, Inc., City of Industry, California 91748, USA

(Received 6 November 2008; accepted 29 December 2008; published online 26 January 2009)

Quantum cascade (QC) laser core heating is a primary impediment to high device wall plug efficiency (WPE). Here, we demonstrate that efficient photon generation produces a quantifiable reduction in heating of the QC laser core temperature. By superimposing low duty cycle current pulses on a core-heating dc baseline, we observe the instantaneous threshold current and current efficiency evolution as the dc input is varied. From these measurements we recover the laser core temperature  $T_{\text{core}}$ . Results agree well with calculations of  $T_{\text{core}}$  based on measured thermal resistance and WPE. Using the same thermal model for a laser with negligible WPE, we show that the large WPE of the measured device—24% for an 80 K heat sink—results in a core temperature reduction of  $\sim 15$  K. © 2009 American Institute of Physics. [DOI: 10.1063/1.3073044]

Recent improvements in quantum cascade (QC) lasers have resulted in devices that operate with large wall plug efficiency (WPE) at both cryogenic and room temperatures.<sup>1–4</sup> This progress has come from better models,<sup>5–7</sup> designs,<sup>1,3,8</sup> and improved thermal management.<sup>1–4,9</sup> Due to conservation of energy, a result of this efficient emission of light is that a substantial fraction of the input electrical power no longer contributes to the heating of the active core. This reduction in heating is highly desirable since elevated core temperatures can dramatically limit QC laser performance to the point of thermal rollover.<sup>5,6</sup> Understanding and harnessing this lasing-induced reduction in heating may enable further improvements in laser performance.

Studies of the thermal behavior of QC lasers using non-invasive methods were previously reported. Scanning interferometric thermal mapping techniques measured both spatial and temporal lattice temperature profiles in QC lasers.<sup>10</sup> Microprobe photoluminescence measurements allowed simultaneous determination of the lattice and electronic temperatures.<sup>11,12</sup> Additionally, using this method, it was shown that threshold currents of QC lasers are determined by the lattice temperature and can be reliably used as a thermometric property of the active core.<sup>12</sup>

Here, we are interested in only the lattice temperature of the QC laser active core because the temperature effects due to large WPE are most observable in this region of the laser. We use the temperature-dependent threshold as an indicator of the active core temperature. For a laser operated in continuous wave (cw) mode, this is accomplished by superimposing low duty cycle pulses on a core-heating dc baseline,<sup>13</sup> measuring the instantaneous threshold current, and relating the result to known threshold versus active core temperature data. Using this measurement technique, we are able to determine the instantaneous core temperature, current efficiency, and reduction in core heating from photon emission.

The lasers used in this study were grown by metal organic chemical vapor deposition using strained  $\text{In}_{0.669}\text{Ga}_{0.331}\text{As}/\text{Al}_{0.638}\text{In}_{0.362}\text{As}$  quantum wells and barriers on an InP substrate with the net strain balanced in each period. The active core is a traditional, high-performance two-phonon resonance design with an engineered optical transition energy of 270 meV similar to that in Ref 1. The devices were processed as buried heterostructure lasers using lateral InP regrowth and mounted epitaxial layer up to a copper holder using indium.

The laser holder was mounted to a copper heat sink in a temperature controlled, continuous flow liquid nitrogen cryostat. Ge lenses were used to collect and focus the light onto a room temperature HgCdTe detector for pulsed measurements and a thermopile for cw measurements. The pulsed measurements were performed using 100 ns pulses at 5 kHz. The results in this letter are for the best performing laser ridge, 3.0 mm long and  $5.2\ \mu\text{m}$  wide, and are characteristic of the several other tested devices. Figure 1 shows results for cw measurements at a heat sink temperature of 80 K. At this heat sink temperature, the device has a threshold current of 165 mA, 24% peak WPE in cw mode, and 33% peak WPE in pulsed mode.

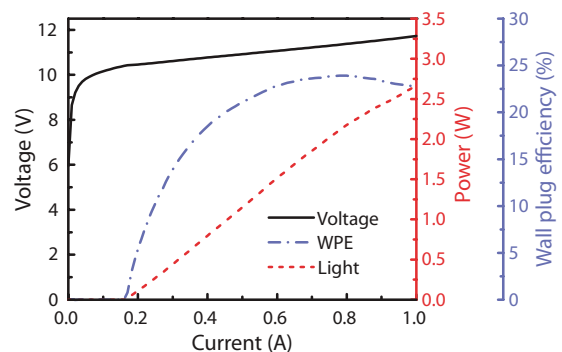


FIG. 1. (Color online) cw voltage (solid, black), light (dash, red), and WPE (dot-dash, blue) vs current curves for the high efficiency device at a heat sink temperature of 80 K. The power and WPE values are reported for both facets.

<sup>a)</sup>Electronic mail: ajhoffma@princeton.edu.

<sup>b)</sup>Present address: Department of Applied and Engineering Physics, Cornell University, Ithaca, NY 14850, USA.

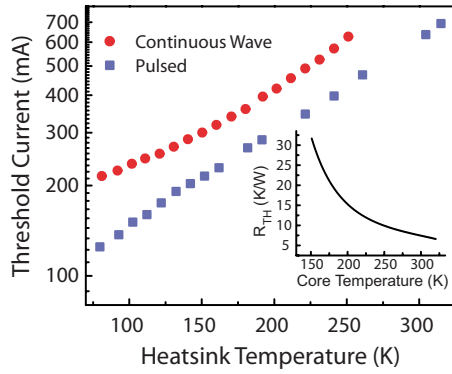


FIG. 2. (Color online) Threshold current vs heat sink temperature data of the high efficiency device for cw (red circles) and pulsed (blue squares) operation. The inset shows the thermal resistance  $R_{th}$  calculated from the difference in threshold currents vs temperature.

Pulsed and cw thresholds as a function of heat sink temperature are shown in Fig. 2. These thresholds were fit using high-order polynomial functions, and the thermal resistance for a given core temperature was calculated as  $R_{TH}(T_{core}) = (T_{th,pulsed} - T_{th,cw}) / (P_{th,cw})$ , where  $T_{th,pulsed}$  is the core temperature at the pulsed threshold,  $T_{th,cw}$  is the core temperature at the cw threshold, and  $P_{th,cw}$  is the input power at cw threshold. The core temperature at cw threshold was determined by matching the temperature for a pulsed measurement with the same threshold current. The calculated thermal resistance is shown in the inset of Fig. 2.

To measure the instantaneous threshold current  $I_{instant}$  of the device during cw operation, the heat sink was cooled to 80 K. The temperature of the heat sink was monitored and controlled; the variation in temperature over the course of the experiment was less than 0.3 K. Light was collected onto a room temperature HgCdTe detector that was preceded by a polarizing filter to limit the amount of incident power. Pulses of 100 ns at 5 kHz were superimposed on a dc current using an impedance-matched bias- $T$ ; the very low duty cycle ensures that the pulses have a negligible effect on the temperature of the core. The center 20 ns of the current and light pulses were gated and averaged over 100 pulses. The magnitude of the low duty cycle pulses was increased every 300 ms (1500 pulses). The laser was designed to operate under negative polarity; thus for dc currents below the cw threshold, negative polarity pulses were used. Above cw threshold, positive polarity pulses were used. The polarity of the pulses was controlled by the inclusion or exclusion of an inverter immediately after the pulse generator. Figure 3 shows measurements below and above cw threshold, and the inset shows a schematic of the supplied pulses. Below cw threshold, the measurements are very similar to typical light-current measurements. However, above cw threshold, the device is turned off as larger pulses are applied. A threshold  $\delta I_{pulse,th}$  is clearly visible for both measurements. The instantaneous threshold current of the device is given by  $I_{instant,th} = I_{dc} + \delta I_{pulse,th}$ , where  $I_{dc}$  is the dc current supplied to the device. The instantaneous current efficiency is given by  $(I_{dc} - I_{instant,th}) / I_{dc}$ .

To study the evolution of the instantaneous threshold at various points of cw operation (active core temperatures), the input dc power was changed and the instantaneous threshold was measured as described above. The change in the dc current was made slowly to avoid temperature fluctuations in

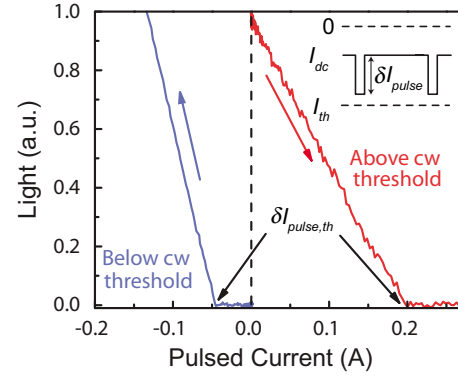


FIG. 3. (Color online) Light vs pulsed current for measurements below (blue) and above (red) cw threshold. The blue and red arrows show the direction of the increase in the magnitude of the current pulses below and above cw threshold, respectively. The inset shows a schematic of the current pulses supplied to the device in addition to the dc current. The lasing threshold  $\delta I_{pulse,th}$  is indicated for both measurements.

the heat sink. The temperature of the heat sink was allowed to stabilize to fluctuations of  $<0.01$  K, and the voltage of the QC laser, an indicator of core temperature, was allowed to stabilize to fluctuations of  $<0.1$  mV before recording a measurement. The maximum dc current applied was limited by the bias- $T$  to 1 A. The minimum was limited to approximately 50 mA due to instability in the voltage for smaller dc currents. The standard deviation of the instantaneous thresholds at each cw current over the entire range of cw data is less than 1 mA. We observed a threshold dependence on the boxcar gate location of approximately 10 mA and estimate the error in our measurements to be approximately  $\pm 5$  mA.

Each of the measured instantaneous thresholds was mapped to a core temperature using the pulsed threshold versus heat sink temperature data shown in Fig. 2. Figure 4 shows the results of the measurements and mapping. Using the WPE and  $R_{TH}$  data, the core temperature was calculated. The starting core temperature of 131 K was selected to match the experimental data at the power corresponding to the onset of cw lasing, 1.8 W; no other fitting parameters were used. For the calculations, the change in core temperature  $\Delta T_{core}$  was calculated as

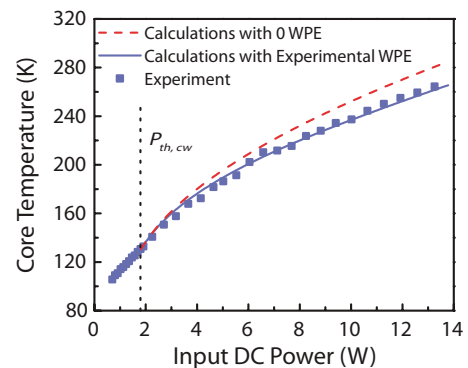


FIG. 4. (Color online) Plot of core temperature vs dc input power. The blue squares are for the experimental results; the blue, solid line is for calculations including the WPE; and the red, dashed line is for calculations with zero WPE for all input powers. The power corresponding to cw threshold,  $P_{dc,th} = 1.8$  W, is marked by the vertical, dashed line. There is excellent agreement between experiment and the calculations; the only free parameter is the initial core temperature, which was matched to the experiment.

$$\Delta T_{\text{core}}(T_{\text{core}}) = \Delta P_{\text{dc}} [1 - \eta_{\text{WPE}}(P_{\text{dc}})] R_{\text{TH}}(T_{\text{core}}),$$

where  $\Delta P_{\text{dc}}$  is the change in applied dc power and  $\eta_{\text{WPE}}$  is the WPE. The increment in core temperature  $\Delta T_{\text{core}}$  was added to the previously calculated temperature. As can be seen in Fig. 4, there is excellent agreement between the experimental data and the calculations.

To show the effect of large  $\eta_{\text{WPE}}$  on the temperature of the core, calculations were performed using the same thermal parameters with  $\eta_{\text{WPE}}=0$  for all dc powers. The results are also shown in Fig. 4. Around  $P_{\text{dc}}=12$  W input power, the difference in core temperature is approximately 15 K. This difference in temperature is due to the efficient emission of light for this device. The size of the temperature difference is strongly influenced by  $R_{\text{TH}}$ , and the reduction in  $R_{\text{TH}}$  at higher core temperatures limits the magnitude of the difference; at  $P_{\text{dc}}=12$  W,  $R_{\text{TH}} \approx 9.3$  K/W.

In conclusion, we have measured the evolution of the core temperature and current efficiency of a QC laser in cw operation. The measured results agree well with calculations of the core temperature that use both the measured  $\eta_{\text{WPE}}$  and  $R_{\text{TH}}$ . Excluding  $\eta_{\text{WPE}}$  in the model results in an increase in the core temperature of 15 K at typical cw operating currents. The size of the temperature difference is strongly influenced by  $R_{\text{TH}}$ .

This work is supported in part by DARPA-EMIL and MIRTHER (Grant No. NSF-ERC EEC-0540832).

- <sup>1</sup>A. Evans, S. R. Darvish, S. Slivken, J. Nguyen, Y. Bai, and M. Razeghi, *Appl. Phys. Lett.* **91**, 071101 (2007).
- <sup>2</sup>Y. Bai, S. R. Darvish, S. Slivken, W. Zhang, A. Evans, J. Nguyen, and M. Razeghi, *Appl. Phys. Lett.* **92**, 101105 (2008).
- <sup>3</sup>A. Lyakh, C. Pflügl, L. Diehl, Q. J. Wang, F. Capasso, X. J. Wang, J. Y. Fan, T. Tanbun-Ek, R. Maulini, A. Tsekoun, R. Go, and C. K. N. Patel, *Appl. Phys. Lett.* **92**, 111110 (2008).
- <sup>4</sup>Y. Bai, S. Slivken, S. R. Darvish, and M. Razeghi, *Appl. Phys. Lett.* **93**, 021103 (2008).
- <sup>5</sup>S. S. Howard, Z. Liu, D. Wasserman, A. J. Hoffman, T. S. Ko, and C. F. Gmachl, *IEEE J. Sel. Top. Quantum Electron.* **13**, 1054 (2007).
- <sup>6</sup>S. S. Howard, Z. Liu, and C. F. Gmachl, *IEEE J. Quantum Electron.* **44**, 319 (2008).
- <sup>7</sup>A. Wittmann, Y. Bonetti, J. Faist, E. Gini, and M. Giovannini, *Appl. Phys. Lett.* **93**, 141103 (2008).
- <sup>8</sup>A. J. Hoffman, S. Scharfner, S. S. Howard, K. J. Franz, F. Towner, and C. Gmachl, *Opt. Express* **15**, 15818 (2007).
- <sup>9</sup>M. Beck, D. Hofstetter, T. Aellen, J. Faist, U. Oesterle, M. Illegems, E. Gini, and H. Melchior, *Science* **295**, 301 (2002).
- <sup>10</sup>C. Pflügl, M. Litzenberger, W. Schrenk, D. Pogany, E. Gornik, and G. Strasser, *Appl. Phys. Lett.* **82**, 1664 (2003).
- <sup>11</sup>V. Spagnolo, M. Troccoli, G. Scamarcio, C. Gmachl, F. Capasso, A. Tredicucci, A. M. Sergent, A. L. Hutchinson, D. L. Sivco, and A. Y. Cho, *Appl. Phys. Lett.* **78**, 2095 (2001).
- <sup>12</sup>V. Spagnolo, G. Scamarcio, H. Page, and C. Sirtori, *Appl. Phys. Lett.* **84**, 3690 (2004).
- <sup>13</sup>S. Katz, A. Friedrich, G. Boehm, and M.-C. Amann, *Appl. Phys. Lett.* **92**, 181103 (2008).